Iğdır Üniversitesi Fen Bilimleri Enstitüsü Dergisi, 13(3), 1713-1723, 2023
Journal of the Institute of Science and Technology, 13(3), 1713-1723, 2023

ISSN: 2146-0574, eISSN: 2536-4618

Physics **DOI: 10.21597/jist.1254573**

Research Article

Received: 21.02.2023 **Accepted: 05.05.2023**

To Cite: Toprak, S. & Serif, R. (2023). Fabrication and Electrical Characterization of $Cu_{1-x}Cr_xO$/n-Si Diodes by Sol Gel Spin Coating Method. *Journal of the Institute of Science and Technology*, 13(3), 1713-1723.

$Cu_{1-x}Cr_xO$/n-Si Diyotlarının Sol Jel Spin Kaplama Yöntemi ile Üretimi ve Elektriksel Karakterizasyonu

Seyhmus TOPRAK[1], Serif RUZGAR[2*]

Öne Çıkanlar:
- $Cu_{1-x}Cr_xO$/n-Si heteroeklem diyotları inşa edildi
- Heteroeklemlerin yapısı düzeltme davranışı sergilemiştir
- Çeşitli frekanslarda birkaç C-V ölçümü, tuzakların varlığını doğrular

Anahtar Kelimeler:
- Sol jel yöntemi
- İnce filmler
- Diyot
- Elektriksel Özellikler

ÖZET:

Katkısız ve Cr katkılı CuO ince filmlerini n-Si alt tabakalar üzerine sol jel spin kaplama yöntemi ile üretildi. Üretilen bu heteroeklem yapıların farklı krom oksit ve bakır oksit karışım oranları için diyotların elektriksel özellikleri incelendi. Sonuçlar, Cr konsantrasyonundaki bir değişikliğin, Ag/$Cu_{1-x}Cr_xO$/n-Si diyotlarının elektriksel özelliklerini önemli ölçüde etkilediğini göstermektedir. Tüm diyotlar, karanlık I-V grafiklerinden de görüleceği üzere düzeltme davranışı sergiledi. Seri direnç (Rs), doğrultma oranı (RR), idealite faktörü (n) ve bariyer yüksekliği (Φ_B) gibi önemli elektriksel parametreleri $I-V$ verileri kullanılarak hesaplandı. Diyotların performansı hakkında ayrıntılar sunan idealite faktörü (n) için hesaplanan değerler 2.16 ile 2.78 arasında değişmektedir. En yüksek RR değeri Cu0.5Cr0.5O/n-Si diyottan elde edilmiştir. Diyotların kapasite-gerilim $C-V$ özellikleri 10 kHz ila 1 MHz frekans aralığında ölçülmüştür. $C^{-2}-V$ grafikleri yardımıyla N_v, E_f, E_{max}, ve Φ_B $(C-V)$ parametreleri hesaplandı. Elde edilen sonuçlar, Ag/$Cu_{1-x}Cr_xO$/n-Si diyotlarının elektriksel özelliklerinin, farklı krom katkılama miktarı ile kontrol edilebileceğini göstermektedir.

Fabrication and Electrical Characterization of $Cu_{1-x}Cr_xO$/n-Si Diodes by Sol Gel Spin Coating Method

Highlights:
- The $Cu_{1-x}Cr_xO$/n-Si heterojunction diodes were constructed
- The structure of the heterojunctions displayed rectification behavior
- C-V measurements at various frequencies confirm the existence of traps

Keywords:
- Sol gel method
- Thin films
- Diode
- Electrical Properties

ABSTRACT:

Undoped and Cr-doped CuO thin films were deposited on *n*-Si substrates by sol gel spin coating method. These electrical properties of copper oxide-based heterojunction structures were examined as a function of Cr doping concentrations. The results show that a change in Cr concentration significantly affects the electrical properties of Ag/$Cu_{1-x}Cr_xO$/n-Si diodes. The all diodes exhibit rectification behavior, as shown by their dark $I-V$ characteristics. The crucial junction parameters such as series resistance (R_S), rectification ratio (RR), ideality factor (n) and barrier height (Φ_B) were calculated by using $I-V$ data. The calculated values for the ideality factor (n), which offered details about the performance of the diodes, range from 2.16 to 2.78. The highest RR value was obtained from $Cu_{0.5}Cr_{0.5}O$/n-Si diode. In addition, the capacitance-voltage $(C-V)$ characteristics of the diodes were measured in the frequency range of 10 kHz and 1 MHz. The $C^{-2}-V$ graphs were employed to calculate the values of N_v, E_f, E_{max}, and Φ_B $(C-V)$. The results show that the electrical properties of Ag/$Cu_{1-x}Cr_xO$/n-Si diodes can be controlled by various chromium doping concentration.

[1] Seyhmus TOPRAK (**Orcid ID:** 0000-0002-1275-8666), Department of Physics, Graduate School of Education, Batman University, Batman, Türkiye
[2] Serif RUZGAR (**Orcid ID:** 0000-0002-4964-2202), Department of Opticianry Program, Vocational School of Health Services, Batman University, Batman, Türkiye

[*]**Corresponding Author:** Serif RUZGAR, e-mail: serif.ruzgar@batman.edu.tr

This study was produced from Seyhmus Toprak's Master's thesis.

INTRODUCTION

Recently, metal oxide semiconductors have emerged as prospective candidates for a variety of electronic and optoelectronic devices such as gas sensors, light-emitting diode displays, photodetectors, and biosensor, thanks to their benefits such as chemical and mechanical stability and low temperature processing (Amde et al., 2017; Ruzgar et al., 2020). The majority of metal oxides employed in optoelectronic device applications, such as ZnO, In_2O_3, WO_3, and TiO_2, have *n*-type semiconductor electrical characteristics (Bera et al., 2016). In order to fabricate heterojunction structures, it is necessary to produce and study *p*-type semiconductor metal oxides as an alternative to *n*-type metal oxides. On the other hand, due to their strong localization, poor stability, and large hole effective mass, *p*-type metal oxide manufacturing is a problem that needs to be solved for optoelectronic device applications (Yin et al., 2020). Therefore, improving the performance of *p*-type semiconductors is vital for optoelectronic applications. For this, intensive studies are carried out to search for suitable *p*-type metal oxide semiconductors in optoelectronic applications. The number of candidate *p*-type metal oxide semiconductors for heterojunction applications is less than their *n*-type counterparts. Among the few natural *p*-type metal oxide semiconductors, copper oxide (Cu_xO) attracts attention due to its advantages such as abundance in nature, non-toxicity and low production cost (Ruzgar, Caglar, Polat, et al., 2021). Besides the advantageous properties of Cu_xO, it also has disadvantages such as high resistivity and low carrier concentration for optoelectronic applications (Masudy-Panah et al., 2015; Ruzgar, Caglar, & Caglar, 2021). In order to overcome such disadvantageous properties, the doping of the host materials with a suitable additive is an efficient technique that offers exceptional flexibility in material modification. Doping metal oxide semiconductors can provide several advantages, such as; enhanced electronic properties, tunable optical properties, improved stability and selective sensing (Yang et al., 2013; Asahi et al., 2001).

The high oxidizing properties of Cr compounds and superior spectroscopic properties such as photoreaction and light polarization manipulation make it a promising candidate as an dopant (Mansour et al., 2021; Peng & Gao, 2008). Therefore, Cr doping will improve the electronic and optoelectronic properties of CuO material and its heterojunction applications. Chromium doped copper oxide thin films are deposited with various methods such as radio frequency (RF) sputtering (Qin et al., 2016), molecular beam epitaxy (Du et al., 2006), ultrasonic spray pyrolysis (Kim et al., 2022) and sol-gel (Zekaik et al., 2019). Among these methods, sol gel draws attention with its advantages such as low temperature applicability, homogeneous and easy doping, thin film thickness control and vacuum-free system (Ruzgar & Pehlivanoglu, 2020).

The aim of this study is to examine the effect of Cr doping on the electrical parameter properties of CuO-based heterojunction diodes by using current-voltage and capacitance-voltage data. Therefore, the undoped and Cr-doped CuO thin films were coated on *n*-Si substrates using inexpensive sol gel technique to fabricate heterojunction structures. The $I-V$ and $C-V$ measurements of these produced diodes were taken in the dark and at room temperature. The electrical characteristics of diodes were investigated as a function of Cr doping. The basic electrical parameters of diodes were examined using conventional Thermionic Emission Theory, Norde method and capacitance-voltage characteristics.

MATERIALS AND METHODS

Sol gel spin coating method was used for the deposition of undoped and Cr doped CuO thin films. While chromium acetate ($Cr(C_2H_3O_2)_3$) and copper acetate ($Cu(CH_3COO)_2$) were used as the source material, 2-Methoxethanol ($C_3H_8O_2$) and monoethanolamine (C_2H_7NO) were utilized as solvent and stabilizer, respectively. 0.05 M solutions of chromium acetate and copper acetate were prepared

and mixed magnetically for two hours at 60ºC. Then, new mixtures were obtained by adding 0%, 25%, 50%, 75% and 100% Cr solution to the CuO solution by volume. The thin films that will be obtained from these solutions are named CuO, $Cu_{0.75}Cr_{0.25}O$, $Cu_{0.50}Cr_{0.50}O$, $Cu_{0.25}Cr_{0.75}O$ and CrO, respectively. In order to produce thin film and fabricate heterojunction, these solutions were coated on *n*-Si substrates with a spin coater with spin parameters of 3000 rpm/30 sec. The *n*-Si substrates were purchased commercially. After each coating, the films were kept in the oven at 300 ºC for 10 min. These processes were repeated 4 times for each sample. Finally, the films were annealed at 350 ºC for 2 hours in the furnace and cooled at room temperature. After the growth of $Cu_{1-x}Cr_xO$ films on *n*-Si substrates, the ohmic contact stage was started for diode production. The fabricated ohmic contacts are circular and 100 nm thick. The current-voltage ($I-V$) and capacitance-voltage ($C-V$) measurements of Ag/$Cu_{1-x}Cr_xO$/n-Si diodes were taken by using Keithley 4800 SCS device in dark condition and room temperature. The fabrication flowchart of the heterojunction structures and the schematic view of the electrical measurement system are shown in Figure 1 (a) and (b).

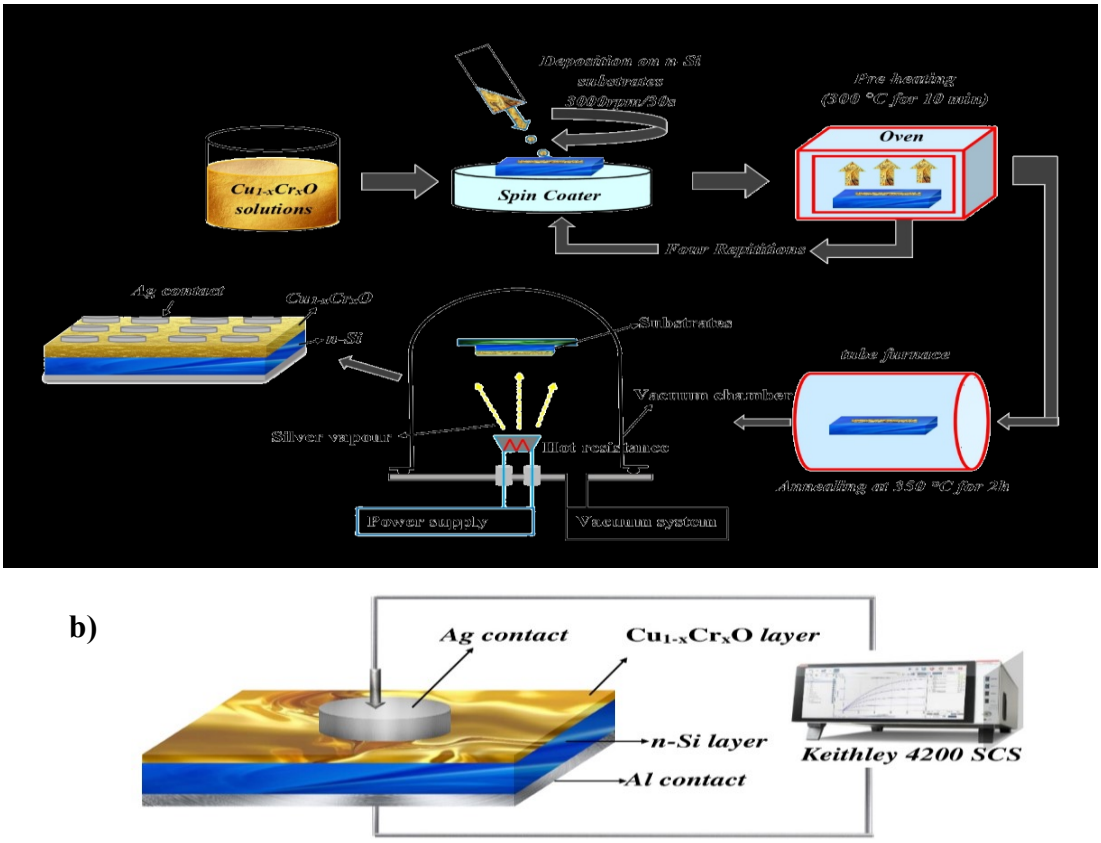

Figure 1. (a) The fabrication flowchart of the heterojunction structures and (b) the schematic representation of the electrical measurement system

RESULTS AND DISCUSSION

The quality of a diode is indicated by the ideality factor (n), which is a non-unit parameter. The ideality factor is equal to 1 for an ideal diode. Thermionic emission (TE) theory are used to calculate the fundamental parameters of diodes, such as the ideality factor. Therefore, TE model was used to analyze the $I-V$ properties of the Ag/$Cu_{1-x}Cr_xO$/n-Si diodes. According to this model (Rhoderick & Williams, 1988), thermionic current and reverse saturation current can be described by following equations;

$$I = I_0\left[exp\left(\frac{q(V-IR_S)}{nkT}\right)-1\right] \quad (1)$$

$$I_0 = AA^*T^2 exp\left(-\frac{q\Phi_B}{kT}\right) \quad (2)$$

Where n is the ideality factor; k is Boltzmann's constant; T is room temperature in Kelvin; q is the charge of the electron, Φ_B is barrier height and V is the applied voltage in forward bias; R_s is the series resistance and I_0 is the saturation current of reverse bias, which is obtained from the intersection of the linear part of the graph $\ln(I) - V$ at zero voltage. The obtained I_0 values for the produced diodes are shown in Table 1. The following equations can be used to get the values of n and Φ_B, which are crucial diode parameters (for $V \geq 3kT/q$);

$$n = \frac{q}{kT}\left(\frac{dV}{d(lnI)}\right) \quad (3)$$

$$\Phi_B = \frac{kT}{q} ln\, ln\left(\frac{A^*AT^2}{I_0}\right) \quad (4)$$

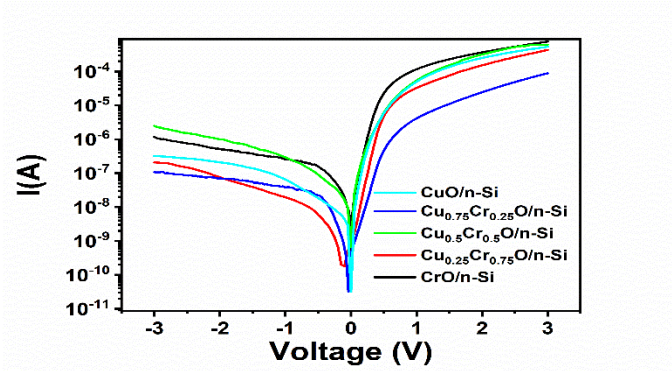

Figure 2. The Semi-Logarithmic I-V Characteristics of Fabricated Ag/$Cu_{1-x}Cr_xO$/n-Si Diode

The semi-logarithmic $I - V$ characteristics of fabricated Ag/$Cu_{1-x}Cr_xO$/n-Si diode is shown in Figure 2. The semi-logarithmic $I - V$ plots of each diode show that the diodes exhibit rectification behavior in the voltage interval of ± 3 V. While the reverse current is weakly dependent on the voltage, the forward current increases exponentially with the applied voltage. As seen in Figure 2, the current-voltage of the diodes show a linear increase in the forward bias region and deviate from linearity due to effects such as ; R_s and interfacial layer.

Table 1. The Electrical Parameters Extracted From $I - V$ Data for the Diodes

Diodes	RR (±3V)	I_0 (A)	n (I-V)	Φ_B (I-V) (eV)	R_s (kΩ)
CuO/n-Si	1.6×10^3	4.58×10^{-9}	2.18	0.78	21.9
$Cu_{0.75}Cr_{0.25}O$/n-Si	2.52×10^2	4.45×10^{-10}	2.78	0.84	46.4
$Cu_{0.50}Cr_{0.50}O$/n-Si	2.07×10^3	8.15×10^{-9}	2.62	0.76	51.6
$Cu_{0.25}Cr_{0.75}O$/n-Si	6.53×10^2	1.03×10^{-9}	2.27	0.81	12.2
CrO/n-Si	18.21×10^2	8.78×10^{-9}	2.16	0.76	4.6

In this study, the maximum rectification ratio value was obtained from $Cu_{0.50}Cr_{0.50}O$/n-Si diode with 2.07×10^3. The RR of a p-n junction is the ratio of the forward current to the reverse current at a given voltage. Doping can affect the rectification ratio by changing the built-in potential of the junction, which is determined by the doping levels of the p and n regions. Increasing the doping concentration of either the p or n region can increase the rectification ratio by increasing the built-in potential. However, excessively high doping levels can lead to lower rectification ratios due to increased leakage current. The calculated n and Φ_B values of the diodes are tabulated in Table 1. The n value is expected to be close to 1 for ideal metal-semiconductor contacts. The n values of all diodes are greater than 1. This shows that the all diodes deviate from ideality. However, deviations from the ideality of these diodes, which are designed as *p-n* heterojunctions, are usually attributed to their

interface state density, the effect of the R_s and the existence of interface layers (Özkartal & Thaer Noori, 2021; Venkateswari et al., 2017). The ideality factor of a p-n junction is a measure of how closely the junction follows ideal diode behavior. It is affected by recombination mechanisms in the junction and is often used to estimate the quality of the junction. Doping can affect the ideality factor by changing the recombination mechanisms in the junction. For example, increasing the doping concentration of the p or n region can increase the ideality factor by reducing recombination in that region. However, doping can also introduce defects that increase recombination, leading to higher ideality factors. The lowest n value was acquired from the CrO/n-Si diode, while the highest Φ_B value, which is another important parameter, was obtained from the $Cr_{0.25}Cu_{0.75}O$/n-Si diode. This results show that the electrical parameters of the diodes can be changed or controlled with the suitable doping concentration. Another key parameter of diodes is series resistance. In Schottky-type devices, the resistance (R_i) is a function of the applied voltage. But when diodes are exposed to sufficiently high voltages, the real value of series resistance becomes visible. The presence of R_s causes bending in both the forward bias of $I-V$ and $C-V$ graphs. The R_s value of the structure can be calculated by using both $I-V$ and $C-V$ values. Ohm's Law, Cheung Function, Norde Method and Nicollian–Brews methods can be performed to calculate the R_s values of the diodes (Cheung & Cheung, 1986; Nicollian & Brews, 2002; Norde, 1979; Sze et al., 2021). Among these methods, the Nicollian–Brews method uses $C-V$ data, while the other three methods use $I-V$ data to calculate the R_s values. Therefore, the modified Norde function can be exploited to calculate the R_s and Φ_B values from a single voltage-dependent current measurement at a constant temperature in this study. Norde functions can be expressed as follows (Norde, 1979);

$$F(V)=\frac{V_0}{\delta}-\frac{kT}{q}ln\left(\frac{I(V)}{A^*AT^2}\right) \quad (5)$$

δ is the first integer value that is greater than the diode's n value. $I(V)$ is the current values obtained from the forward bias of the $I-V$ curve.

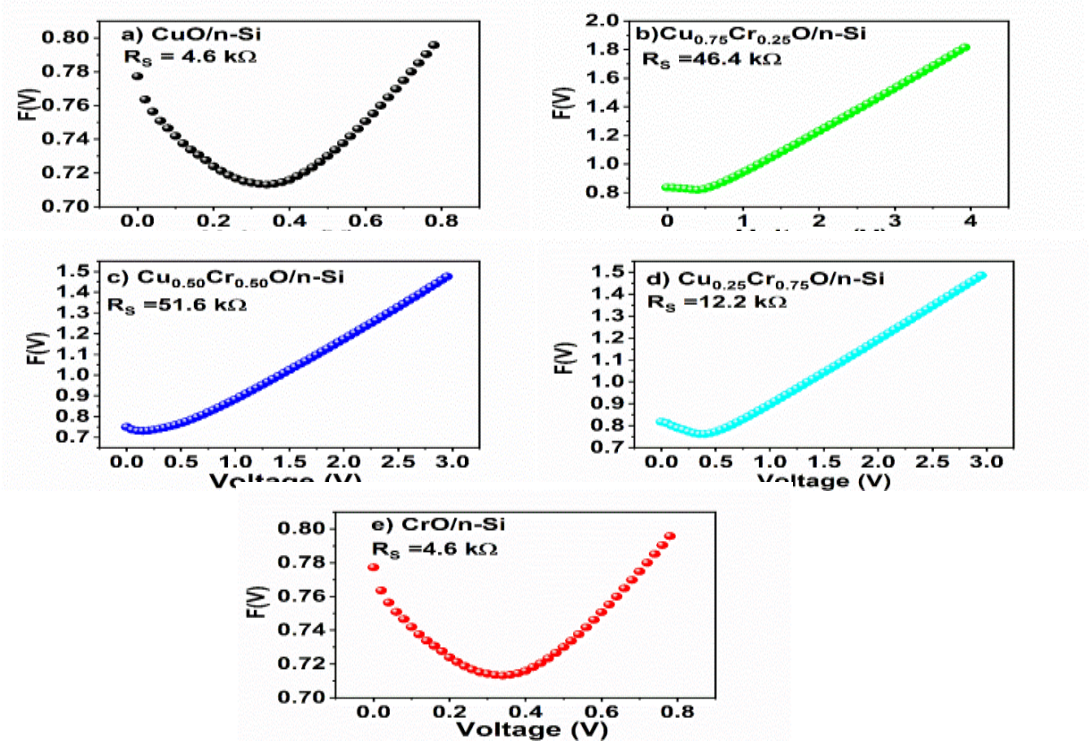

Figure 3. The Modified Norde Graph of Ag/$Cu_{1-x}Cr_xO$/n-Si Diodes

The graph of $F(V) - V$ for Ag/$Cu_{1-x}Cr_xO$/n-Si diodes are shown in Figure 3. The R_s and Φ_B values of the diodes can be defined by using the following equations;

$$\Phi_B = F(V_0) + \frac{V_0}{\delta} - \frac{kT}{q} \quad (6)$$

$$R_s = \frac{kT(\gamma - n)}{qI_0} \quad (7)$$

The diode parameters were calculated by determining the $F(V_0)$, I_0 and V_0 values corresponding to the minimum value of the $F(V)$. The n value, which is obtained from the $I - V$ method, was used, while the R_s values were determined. The calculated series resistance values according to the modified Norde functions are shown in Table 1. The minimum R_s value was obtained from CrO/n-Si diode. Series resistance in a diode can arise from different sources. Some of these reasons are the semiconductor resistance, the contact resistance of the metals, which deposited on the semiconductor, the distribution of the interface states, the existence of SiO_2 oxide layer between the semiconductor and Silicon wafer (Güçlü et al., 2019; Ilican et al., 2016). Diodes with low R_s values are preferred for their practical applications. The $C - V$ characteristics of the Ag/$Cu_{1-x}Cr_xO$/n-Si diodes have been plotted in the ±5V range and shown in Figure 4. The capacitance values of the diodes declined with increment frequency. This is attributed to the existence of interface states (Nss) with various lifetimes in the literature (Güçlü et al., 2019, s. 7; Nicollian & Brews, 2002). The interface states can follow the externally applied AC signal at low frequencies, while it cannot follow at high frequencies. In this case, high values of capacitance are attributed to the additional capacitance, which is resulting from the existence of interface states in the heterostructure (Aydin et al., 2015; Caglar et al., 2016).

The Hill-Coleman theorem is utulized to compute the density of interface states (Dit) from the Gm and Cm data in order to better comprehend these observations (Hill & Coleman, 1980).

$$D_{it} = \frac{2}{qA}\left[\frac{(G_{adj}/w)_{max}}{[(G_{max}/wC_{ox})^2 + (1 - C_m/C_{ox})^2]}\right] \quad (8)$$

Where, Cm, Cox, ω and A symbolize measured capacitance, capacitance of dielectric layer, angular frequency and contact area of the diode, respectively. Equation 8 was used to compute the diode's Dit values, and Figure 5 displays the $Dit - V$ graphs. The density of interface states changes with frequency, as shown in Figure 5, and declines as frequency rises. The decrease is caused by a reduction in the contribution of carriers at the interface at high frequencies (Nicollian & Brews, 2002; Tuğluoğlu et al., 2022). The reverse bias $C^{-2} - V$ graphs at 1 MHz were figured and shown in Figure 6 to obtain the fundamental electronic properties of the diodes such as doping concentration atoms (N_A or N_D), build in potential (V_{bi}), maximum electric field (E_{max}) and the bulk Fermi level (E_f). The relationship between capacitance and voltage for these structures can be defined as follows (Rhoderick & Williams, 1988; Türk et al., 2020);

$$\frac{1}{C^2} = \frac{2(V_{bi} + V)}{A^2 \varepsilon_s q N_D} \quad (9)$$

where ε_s , A, and V_{bi} stand for the semiconductor's permittivity, contact area and the built-in potential, respectively. The intercept and slope of the $C^{-2} - V$ graphs are used to calculate the values of N_V, E_f, E_{max}, and $\Phi_B(C - V)$ for diodes by performing following equations;

$$\Phi_{B(C-V)} = \frac{V_{bi}}{n} + \frac{kT}{q}\ln\left(\frac{N_C}{N_D}\right) \quad (10)$$

$$E_f = \left(\frac{kT}{q}\right)\ln\left(\frac{N_C}{N_D}\right) \quad (11)$$

where N_c represents the effective charge density and is given by (Abdel-Khalek et al., 2018):

$$N_C = 4.82 \times 10^{15} T^{3/2} \left(\frac{m_e^*}{m_0}\right) \quad (12)$$

where m_e^* is the effective mass of the electron and equals 0.98 m_0, while m_0 is the rest mass of the electron. The calculated electrical parameters with using these equations are tabulated in Table 2.

Table 2. The Electrical Parameters Extracted From C-V Data for the Diodes

Diodes	Nd (cm^{-3})	V_{bi} (eV)	Nc (cm^{-3})	Ef (eV)	Φ_B eV (C-V)	Emax (kV/cm)
CuO/n-Si	$2.23x10^{16}$	0.96	$2.38x10^{19}$	0.18	1.17	81.48

Table 2. The Electrical Parameters Extracted From C-V Data for the Diodes(contuined)

$Cu_{0.75}Cr_{0.25}O$/n-Si	$2.15x10^{16}$	1.12	$2.38x10^{19}$	0.18	1.33	86.14
$Cu_{0.50}Cr_{0.50}O$/n-Si	$2.85x10^{15}$	1.60	$2.38x10^{19}$	0.23	1.85	37.50
$Cu_{0.25}Cr_{0.75}O$/n-Si	$4.93x10^{16}$	0.78	$2.38x10^{19}$	0.16	0.97	109.34
CrO/n-Si	$1.11x10^{16}$	1.06	$2.38x10^{19}$	0.20	1.28	60.31

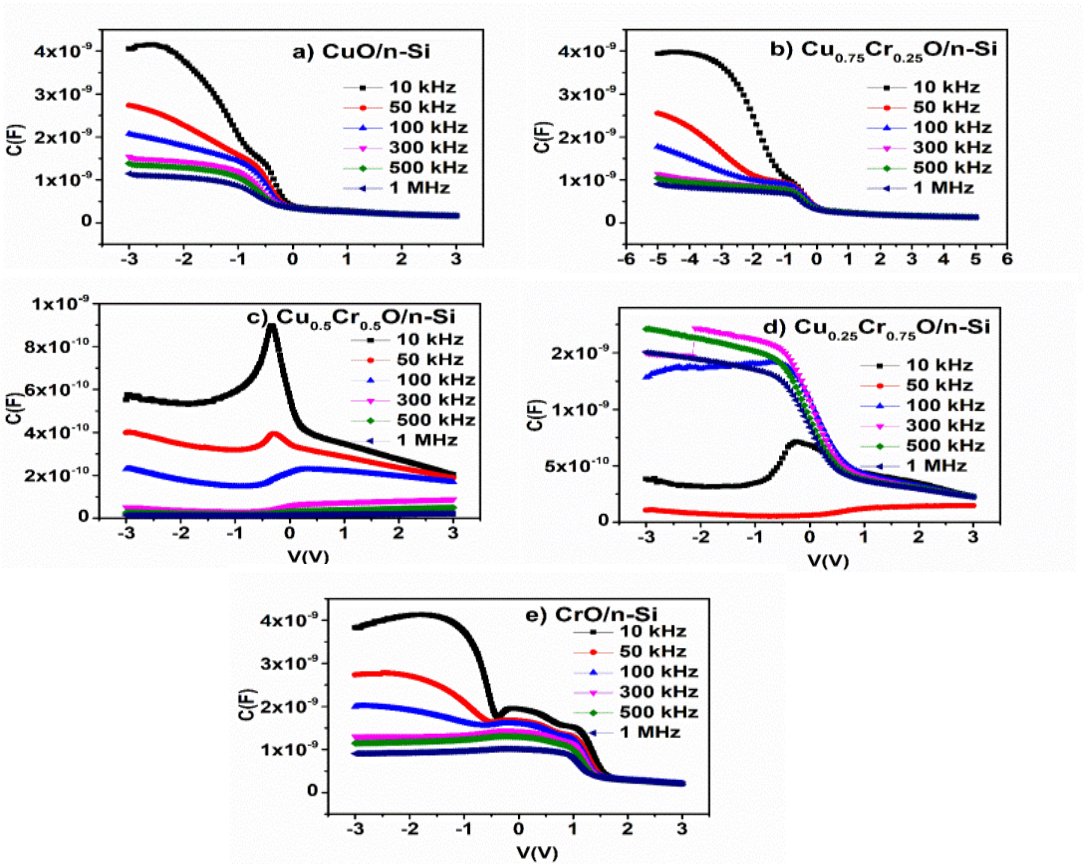

Figure 4. The Capacitance-Voltage Characteristics of the Ag/$Cu_{1-x}Cr_xO$/n-Si Diodes

It is tracked that the barrier height values, which are obtained by the $I-V$ and the $C-V$ method, are different from each other. Also, in general, the barrier height obtained from $C-V$ measurements is greater than that obtained from $I-V$ measurements.

This case is generally attributed to the different nature of both measurement techniques, interface states, image force, barrier inhomogeneities, impurity level, technique of measuring systems and interfacial layer between thin film and Si substrate (Abdel-Khalek et al., 2018; Ahmed et al., 2019; Sze et al., 2021). In addition, as the doping level increases, the obtained barrier height from the $I-V$ measurements decreases, while the obtained barrier height from the $C-V$ measurements remains constant (Tung, 2001). Also, the obtained values of barrier height from $I-V$ or $C-V$ methods are regarded as approximations due to the non-ideality of the diodes.

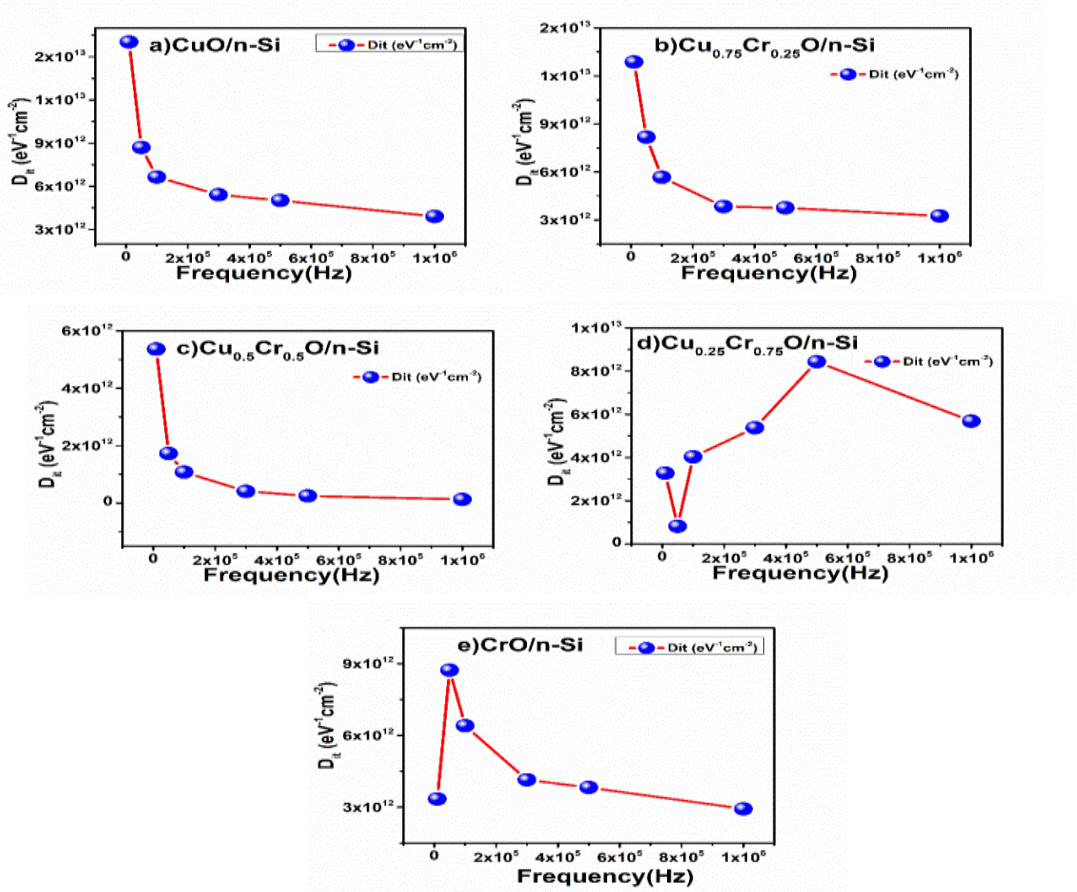

Figure 5. The Density of States–Frequency (Dit-f) Characteristics of the Ag/$Cu_{1-x}Cr_xO$/n-Si Diodes

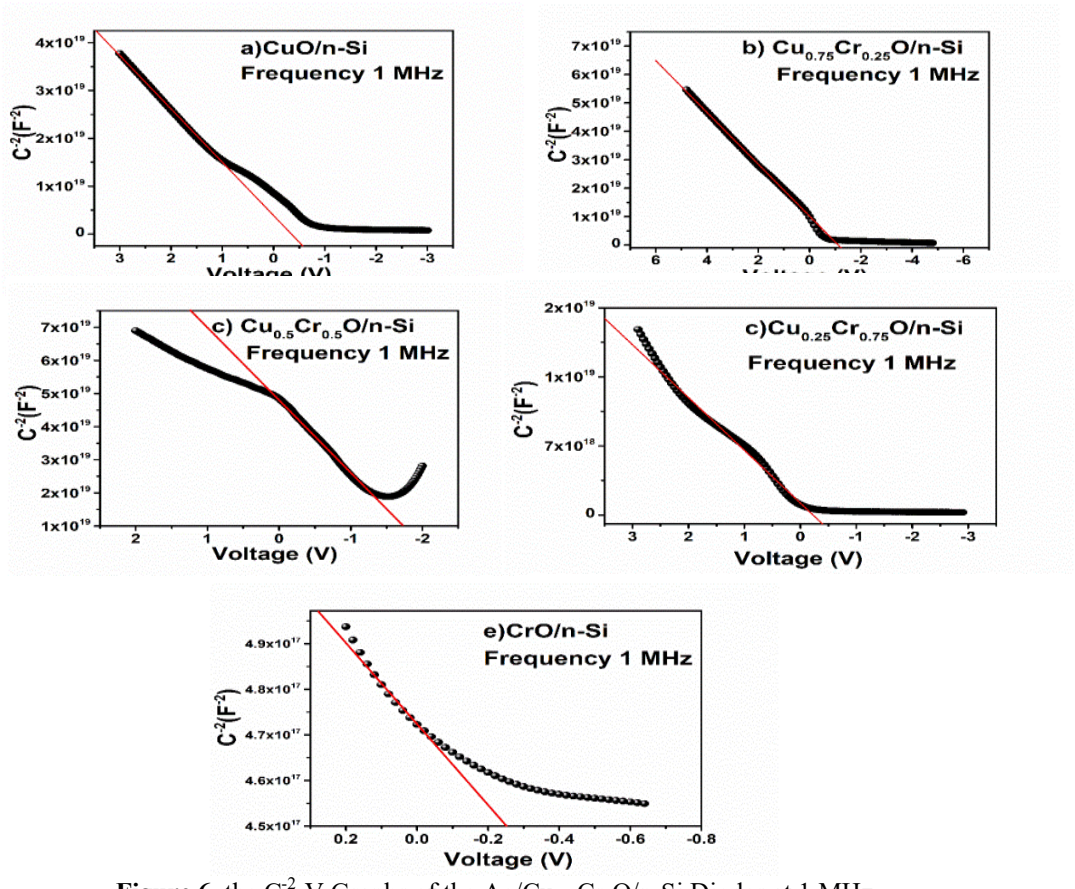

Figure 6. the C^{-2}-V Graphs of the Ag/$Cu_{1-x}Cr_xO$/n-Si Diodes at 1 MHz

CONCLUSION

In this work, $Cu_{1-x}Cr_xO$/n-Si diodes were fabricated to produce an ideal diode with low ideality factor and high barrier height. Low leakage current, good rectification ratio and high barrier height value are obtained for Ag/ $Cu_{1-x}Cr_xO$/n-Si diodes. These results have showed that Cr doping is an attractive method to obtain high performance for CuO/n-Si heterojunction diodes. The calculated values for the ideality factor (n), which offered details about the performance of the diodes, range from 2.16 to 2.78. The highest RR value was obtained from $Cu_{0.5}Cr_{0.5}O$/n-Si diode. In addition, the $C-V$ characterizations of the diodes were scrutinized. The $C-V$ measurements of the diodes have revealed that the capacitance, conductance and series resistance values depend on the frequency. The $C^{-2}-V$ graphs were employed to calculate the values of N_v, E_f, E_{max}, and Φ_B $(C-V)$. In this study, it has been indicated that the electrical characteristic of the Ag/$Cu_{1-x}Cr_xO$/n-Si diodes can be improved and controlled with the appropriate dopant amount.

ACKNOWLEDGEMENTS

This study was supported by Batman University Commission of Scientific Research Project under Grant No. BTUBAP-2019-SHMYO-01

Conflict of Interest

The article authors declare that there is no conflict of interest between them.

Author's Contributions

The authors declare that they have contributed equally to the article.

REFERENCES

Abdel-Khalek, H., Shalaan, E., Abd-El Salam, M., & El-Mahalawy, A. M. (2018). Effect of illumination intensity on the characteristics of Cu(acac)2/n-Si photodiode. Synthetic Metals, 245, 223-236. https://doi.org/10.1016/j.synthmet.2018.09.009

Ahmed, M. A. M., Meyer, W. E., & Nel, J. M. (2019). Effect of (Ce, Al) co-doped ZnO thin films on the Schottky diode properties fabricated using the sol-gel spin coating. Materials Science in Semiconductor Processing, 103, 104612. https://doi.org/10.1016/j.mssp.2019.104612

Amde, M., Liu, J., Tan, Z.-Q., & Bekana, D. (2017). Transformation and bioavailability of metal oxide nanoparticles in aquatic and terrestrial environments. A review. Environmental Pollution, 230, 250-267. https://doi.org/10.1016/j.envpol.2017.06.064

Asahi, R., Morikawa, T., Ohwaki, T., Aoki, K., & Taga, Y. (2001). Visible-light photocatalysis in nitrogen-doped titanium oxides. Science, 293(5528), 269-271.

Aydin, H., Tataroğlu, A., Al-Ghamdi, A. A., Yakuphanoglu, F., El-Tantawy, F., & Farooq, W. A. (2015). A novel type heterojunction photodiodes formed junctions of Au/LiZnSnO and LiZnSnO/p-Si in series. Journal of Alloys and Compounds, 625, 18-25. https://doi.org/10.1016/j.jallcom.2014.11.035

Bera, A., Deb, K., Chattopadhyay, K. K., Thapa, R., & Saha, B. (2016). Mixed phase delafossite structured p type CuFeO2/CuO thin film on FTO coated glass and its Schottky diode characteristics. Microelectronic Engineering, 162, 23-26. https://doi.org/10.1016/j.mee.2016.04.020

Caglar, Y., Görgün, K., Ilican, S., Caglar, M., & Yakuphanoğlu, F. (2016). Magnesium-doped zinc oxide nanorod–nanotube semiconductor/p-silicon heterojunction diodes. Applied Physics A, 122(8), 733. https://doi.org/10.1007/s00339-016-0251-0

Cheung, S. K., & Cheung, N. W. (1986). Extraction of Schottky diode parameters from forward current-voltage characteristics. Applied Physics Letters, 49(2), 85-87. https://doi.org/10.1063/1.97359

Du, X. S., Hak, S., Hibma, T., Rogojanu, O. C., & Struth, B. (2006). X-rays diffraction on a new chromium oxide single-crystal thin film prepared by molecular beam epitaxy. Journal of Crystal Growth, 293(1), 228-232. https://doi.org/10.1016/j.jcrysgro.2006.05.013

Güçlü, Ç. Ş., ÖzdemiR, A. F., & AldemiR, D. A. (2019). Mo/n-Si Schottky Diyotların Akım-Voltaj ve Kapasite-Voltaj Karakteristiklerinin Analizi. Düzce Üniversitesi Bilim ve Teknoloji Dergisi, 7(3), 2142-2155. https://doi.org/10.29130/dubited.544197

Hill, W. A., & Coleman, C. C. (1980). A single-frequency approximation for interface-state density determination. Solid-State Electronics, 23(9), 987-993. https://doi.org/10.1016/0038-1101(80)90064-7

Ilican, S., Caglar, M., Aksoy, S., & Caglar, Y. (2016). XPS Studies of Electrodeposited Grown F-Doped ZnO Rods and Electrical Properties of p-Si/n-FZN Heterojunctions. Journal of Nanomaterials, 2016, e6729032. https://doi.org/10.1155/2016/6729032

Kim, J., Kendall, O., Ren, J., Murdoch, B. J., McConville, C. F., van Embden, J., & Della Gaspera, E. (2022). Highly Conductive and Visibly Transparent p-Type CuCrO2 Films by Ultrasonic Spray Pyrolysis. ACS Applied Materials & Interfaces, 14(9), 11768-11778. https://doi.org/10.1021/acsami.1c24023

Mansour, A. M., Abou Hammad, A. B., & El Nahrawy, A. M. (2021). Sol–gel synthesis and physical characterization of novel MgCrO4-MgCu2O3 layered films and MgCrO4-MgCu2O3/p-Si based photodiode. Nano-Structures & Nano-Objects, 25, 100646. https://doi.org/10.1016/j.nanoso.2020.100646

Masudy-Panah, S., Radhakrishnan, K., Tan, H. R., Yi, R., Wong, T. I., & Dalapati, G. K. (2015). Titanium doped cupric oxide for photovoltaic application. Solar Energy Materials and Solar Cells, 140, 266-274. https://doi.org/10.1016/j.solmat.2015.04.024

Nicollian, E. H., & Brews, J. R. (2002). MOS (Metal Oxide Semiconductor) Physics and Technology. John Wiley & Sons.

Norde, H. (1979). A modified forward I-V plot for Schottky diodes with high series resistance. Journal of Applied Physics, 50(7), 5052-5053. https://doi.org/10.1063/1.325607

Özkartal, A., & Thaer Noori, D. (2021). Ni/n-GaAs ve NiO/n-GaAs Diyotların Elektriksel Parametreleri Arasındaki İlişki. Bitlis Eren Üniversitesi Fen Bilimleri Dergisi. https://doi.org/10.17798/bitlisfen.879884

Peng, C., & Gao, L. (2008). Optical and Photocatalytic Properties of Spinel ZnCr2O4 Nanoparticles Synthesized by a Hydrothermal Route. Journal of the American Ceramic Society, 91(7), 2388-2390. https://doi.org/10.1111/j.1551-2916.2008.02417.x

Qin, P.-L., Lei, H.-W., Zheng, X.-L., Liu, Q., Tao, H., Yang, G., Ke, W.-J., Xiong, L.-B., Qin, M.-C., Zhao, X.-Z., & Fang, G.-J. (2016). Copper-Doped Chromium Oxide Hole-Transporting Layer for Perovskite Solar Cells: Interface Engineering and Performance Improvement. Advanced Materials Interfaces, 3(14), 1500799. https://doi.org/10.1002/admi.201500799

Rhoderick, E. H., & Williams, R. H. (1988). Metal-semiconductor Contacts. Clarendon Press.

Ruzgar, S., Caglar, Y., & Caglar, M. (2021). The optoelectrical properties of rare earth element Eu doped CuxO based heterojunction photodiode. Chinese Journal of Physics, 72, 587-597. https://doi.org/10.1016/j.cjph.2021.05.017

Ruzgar, S., Caglar, Y., Polat, O., Sobola, D., & Caglar, M. (2020). The tuning of electrical performance of Au/(CuO:La)/n-Si photodiode with La doping. Surfaces and Interfaces, 21, 100750. https://doi.org/10.1016/j.surfin.2020.100750

Ruzgar, S., Caglar, Y., Polat, O., Sobola, D., & Caglar, M. (2021). The influence of Fe substitution into photovoltaic performance of p-CuO/n-Si heterojunctions. Journal of Materials Science: Materials in Electronics, 32(15), 20755-20766. https://doi.org/10.1007/s10854-021-06589-9

Ruzgar, S., & Pehlivanoglu, S. A. (2020). The effect of Fe dopant on structural, optical properties of TiO2 thin films and electrical performance of TiO2 based photodiode. Superlattices and Microstructures, 145, 106636. https://doi.org/10.1016/j.spmi.2020.106636

Sze, S. M., Li, Y., & Ng, K. K. (2021). Physics of Semiconductor Devices. John Wiley & Sons.

Tuğluoğlu, N., Taşcı, E., & Eymur, S. (2022). ANALYSIS OF INTERFACE TRAPS OF Au/C25H25BF2N2O/n-Si SCHOTTKY DIODES BY HILL-COLEMAN TECHNIQUE. NEW MATERIALS, 10.

Tung, R. T. (2001). Recent advances in Schottky barrier concepts. Materials Science and Engineering: R: Reports, 35(1), 1-138. https://doi.org/10.1016/S0927-796X(01)00037-7

Türk, Ç. G., Tan, S. O., Altındal, Ş., & İnem, B. (2020). Frequency and voltage dependence of barrier height, surface states, and series resistance in Al/Al2O3/p-Si structures in wide range frequency and voltage. Physica B: Condensed Matter, 582, 411979. https://doi.org/10.1016/j.physb.2019.411979

Venkateswari, P., Thirunavukkarasu, P., Ramamurthy, M., Balaji, M., & Chandrasekaran, J. (2017). Optimization and characterization of CuO thin films for P–N junction diode application by JNSP technique. Optik, 140, 476-484. https://doi.org/10.1016/j.ijleo.2017.04.039

Yang, J., Wang, D., Han, H., & Li, C. A. N. (2013). Roles of cocatalysts in photocatalysis and photoelectrocatalysis. Accounts of chemical research, 46(8), 1900-1909.

Yin, W., Yang, J., Zhao, K., Cui, A., Zhou, J., Tian, W., Li, W., Hu, Z., & Chu, J. (2020). High Responsivity and External Quantum Efficiency Photodetectors Based on Solution-Processed Ni-Doped CuO Films. ACS Applied Materials & Interfaces, 12(10), 11797-11805. https://doi.org/10.1021/acsami.9b18663

Zekaik, A., Benhebal, H., & Benrabah, B. (2019). Synthesis and characterization of Cu doped chromium oxide (Cr2O3) thin films. High Temperature Materials and Processes, 38(2019), 806-812. https://doi.org/10.1515/htmp-2019-0037